Brazilian Journal of Chemical Engineering (2021) 38:197–214
https://doi.org/10.1007/s43153-020-00084-0

ORIGINAL PAPER

Chemical exergy influence in the exergetic analysis of a real clinker rotary kiln

Túlio Franco Anacleto[1] · Ana Esther Gonçalves de Oliveira e Silva[1] · Suzimara Reis da Silva[1] · Esly Ferreira da Costa Junior[1] · Andréa Oliveira Souza da Costa[1]

Received: 6 May 2020 / Revised: 17 December 2020 / Accepted: 19 December 2020 / Published online: 10 January 2021

Abstract

The most energy demanding process in the cement industry is clinker production, carried out in a rotary kiln. Thus, rotary kiln energetic and exergetic analyses are useful tools to reach cement production process improvements. Energetic analysis is based on the first law of thermodynamics and allows one to calculate the heat uses and losses. On the other hand, exergetic analysis is based on a combination of the First and Second Laws of Thermodynamics and allows quantifying process irreversibilities. Some rotary kiln exergy analyses neglect the mass flows chemical exergy in the exergetic analysis, considering only the fuel chemical exergy. In this work, chemical exergy impact on this analysis was evaluated. Pre-calcination effect was also studied. Rotary kiln classical and modern exergetic efficiency considering all the chemical exergy contributions were 55.5% and 41.8%, respectively, while considering just the fuel chemical exergy were 38.2% and 22.6%, respectively. The results showed that it is inadequate to neglect the mass flows chemical exergy, since their contribution in the exergetic analysis was relevant. Furthermore, it was observed that the method adopted in the process efficiency evaluation affects the system interpretation. Considering the modern exergetic efficiency, results showed that, the higher the pre-calcination, the higher rotary kiln efficiency.

Keywords Energy · Exergy · Efficiency · Calcination · Cement · Clinker

List of symbols

A	Fuel mass percentage of ash in dry basis
c_i	Element fraction appearing in the form of the reference species.
c_p	Heat capacity at constant pressure (J/mol.K)
C	Fuel mass percentage of carbon in dry basis.
E	Energy (kJ)
$\dot{E}$	Energy rate (kJ/h)
ex	Specific exergy (J/mol)
ex^0_{ch}	Specific standard chemical exergy (J/mol)
Ex	Exergy (kJ)
$\dot{E}$	Exergy rate (kJ/h)
g	Gravitational acceleration (m/s^2)
g^0_f	Standard Gibbs energy of formation (J/mol)
h	Specific Enthalpy (J/mol)
h^0_f	Specific Enthalpy of formation (J/mol)
H	Fuel mass percentage of hydrogen in dry basis.
j	Number of reference ions or molecules derived from one molecule of the element under consideration.
l_i	Number of atoms of the element in the molecule of the reference species.
$\dot{m}$	Mass flow rate (kg/h)
M_0	Lithosphere molecular mass (kg/mol)
$n_{i,0}$	Lithosphere molar concentration of the ith element.
N	Fuel mass percentage of Nitrogen in dry basis.
N_k	Number of molecules of additional elements present in the molecule of the reference species.
O	Fuel mass percentage of oxygen in dry basis.
P	Pressure (atm)
pH	Negative logarithm of the hydrogen ion concentration.
$\dot{Q}$	Heat transfer rate (kJ/h)
R	Universal gas constant. (J/mol.K)
s	Specific Entropy (J/mol.K)
S	Coal mass percentage of sulfur in dry basis.
T	Temperature (K)

✉ Andréa Oliveira Souza da Costa
andreacosta@deq.ufmg.br

[1] Chemical Engineering Program, Departamento de Engenharia Química, Universidade Federal de Minas Gerais, Av. Presidente Antônio Carlos, Belo Horizonte, Minas Gerais 662731270-901, Brazil

u_0 Conventional standard molar concentration of the reference species in seawater.
v Velocity (m/s)
$\dot{W}$ Power (W)
x Mass fraction.
z Position

Greek letters

α Heat capacity at constant pressure parameter. (*)
β Heat capacity at constant pressure parameter. (*)
δ Heat capacity at constant pressure parameter. (*)
ε Heat capacity at constant pressure parameter. (*)
γ Activity coefficient.
η_{en} Energetic Efficiency.
η_{ex} Exergetic Efficiency.
μ Chemical potential. (J/mol)
σ Heat capacity at constant pressure parameter. (*)
ν Stoichiometric coefficient.
χ_i Reference specie mole fraction in the lithosphere
* The heat capacity at constant pressure parameters have different units as a function of the heat capacity equation. For each equation, the parameters units are defined in such a way that the heat capacity has the unit (J/mol.K).

Subscripts

0 Restricted dead state.
00 Absolute dead state.
ch Chemical.
i Specie.
r Reaction.
d Destroyed.
el Element.

Introduction

The global cement production in the year of 2017 was estimated to be 4.1 billion tons of cement, according to the most recent data of The European Cement Association (Cembureau 2019). The most energy demanding step in cement production is clinker production, carried out in a rotary kiln (Atmaca and Yumrutaş 2014b). According to the World Business Council For Sustainable Development, the world average thermal energy consumption related to clinker production in the year of 2016 was 3540 MJ per ton of clinker (WBCSD 2016). Consequently, the process energy analysis is relevant in clinker production in order to detect possible energy saving improvements.

In this context, energetic and exergetic analysis can be used to improve the operational conditions of the clinker rotary kiln. The energetic analysis is based on the first law of thermodynamics and allows quantifying the process heat loss and energetic efficiency (Anacleto et al. 2018; Atmaca and Yumrutas 2014; Çamdali et al. 2004; Fellaou and Bounahmidi 2017; Kabir et al. 2010). However, the energetic analysis does not identify the process irreversibilities. This analysis disregards information about the process energy degradation related to the process entropy generation (Fraga et al. 2018; Madlool et al. 2012). This information is necessary to determine the real process energy available to produce work (Costa 2016). Therefore, the energetic efficiency value is unable to give a full comprehension of the process efficiency. On the other hand, exergetic analysis considers the combination of the First and the Second Law of Thermodynamics (Ramos et al. 2019; Yildirim and Genc 2017; Zhao et al. 2018). Thus, this analysis describes the process irreversibilities. Consequently, the exergetic analysis allows locating and quantifying the process energy losses related to the entropy generation (Yildirim and Genc 2017).

A combination of the energetic and exergetic analysis in order to evaluate the performance of rotary kilns has been applied widely and can be found in many works on the literature (Atmaca and Yumrutas 2014; Atmaca and Yumrutaş 2014a, 2014b; Çamdali et al. 2004; Fellaou and Bounahmidi 2017; Gürtürk and Oztop 2014; Renó et al. 2013; Shahin et al. 2016; Ustaoglu et al. 2017). However, the methodologies adopted for this analysis in the different studies are not uniform. There are divergences in the way researchers perform both analyses, especially in the exergetic one. Usually the divergences are seen in the exergy flow and exergetic efficiency calculation. Some authors neglect the chemical exergy contribution to the exergy flow calculation. For the exergetic efficiency calculation, some authors perform the calculation in a classical way, considering the ratio between the outlet flows exergy and the total inlet exergy (Çamdali et al. 2004; Atmaca and Yumrutas 2014). On the other hand, some authors define the exergetic efficiency by the ratio between the desired products exergy and the fuel exergy (or exergy used to drive the process). This is a modern concept of exergetic efficiency (Fellaou and Bounahmidi 2018; Lazzaretto and Tsatsaronis 2006; Madlool et al. 2012; Renó et al. 2013).

Çamdali et al. (2004) describe an energy and exergy analysis for a rotary kiln used in a cement dry process with pre-calcination. In the energy analysis, the energy associated with each rotary kiln stream was accounted for by the sum of two contributions: substance enthalpy of formation and the enthalpy related to the substance temperature (different from the environment temperature), calculated from the substance heat capacity at constant pressure. In relation to the exergy analysis, the proposed exergy balance neglected part of the flows chemical exergy. In fact, except from the fuel chemical exergy, flow chemical exergy was not taken into account. Çamdali et al. (2004) found an energetic efficiency of 97% and an exergetic efficiency of 64.4%. The exergetic efficiency was calculated by the classical approach. The

energetic efficiency obtained is considerably higher than the usual rotary kiln energetic efficiencies in the literature. This is probably a result of the different methodology adopted in the energetic evaluation.

Renó et al. (2013) developed an analysis for a cement pyro processing unit, including the rotary kiln, operating with waste fuel and mineralizer. This work focused on the system exergy analysis. The exergy balance was performed by taking into account the whole chemical exergy contribution, even the flow chemical exergy. Two case studies involving different proportions of alternative and conventional fuel were evaluated. In both cases, the exergetic efficiency was close to 30%. The exergetic efficiency was calculated by the ratio between the clinker exergy and the fuels exergy (modern approach).

Atmaca and Yumrutas (2014) performed an energy and exergy analysis for a rotary kiln in a Turkish cement industry. The energy of each rotary kiln mass flow was evaluated taking into consideration only the temperature contribution (excluding the enthalpy of formation contribution). Then, the flow energy was calculated considering the substance temperature and its heat capacity at constant pressure. The majority of rotary kilns energy evaluation adopt this approach. On the other hand, the exergy analysis of this work was performed disregarding the rotary kiln flows chemical exergy, considering only the fuel chemical exergy. The rotary kiln energetic efficiency was 55.8%, while the exergetic efficiency was 38.7% for the process. Exergetic efficiency was calculated in the classical way.

Ustaoglu et al. (2017) made an energy and exergy analysis for a wet type rotary kiln. The flow chemical exergy was considered in the study. Due to the wet process, the efficiencies calculated were inferior than in similar studies. The rotary kiln presented an energetic efficiency of 46% and an exergetic efficiency of 35%. The exergetic efficiency was calculated by the classical approach. The Ustaoglu et al. (2017) data analysis pointed out that the flow chemical exergy makes a relevant contribution to the total system exergy.

Fellaou and Bounahmidi (2018) performed an exergy analysis for a cement plant. Exergy balance considered the chemical exergy associated with the chemical reactions, but disregarded the process flow chemical exergies. These authors adopted the modern concept of exergetic efficiency. Outlet exergies involved in the system were divided into the following groups: useful exergy, waste exergy and destroyed exergy. First group corresponds to the desired process products exergies. The second group is composed of the undesired system outlet exergies, such as the exergy from outlet flows that are not desired products in the process (exergy unused and unrecovered in the process) and the exergy losses associated with heat loss. The third group corresponds to the system irreversibilities. Therefore, exergetic efficiency was defined as the ratio between the useful exergy and the total inlet exergy, in order to evaluate how efficiently the input exergy was converted in the desired product exergy. This cement plant rotary kiln efficiency was evaluated in 63.09%.

In the present study, the energy and exergy analyses of a real rotary kiln used for clinker production operating with pre-calcination were performed. The energy analysis followed the most common adopted methodology for this system. However, the exergy analysis was performed considering and neglecting the flow chemical exergy contribution, in order to detect the difference between these two approaches. The major aim of this study is to explore the chemical exergy impact on the rotary kiln exergy analysis. Since the rotary kiln is an equipment that involves flows at temperatures considerably elevated, a high impact of chemical exergy in this system indicates that chemical exergy may be considered in any system with reactions and change of streams composition, even in systems involving high temperatures. In addition, the effect of pre-calcination on the rotary kiln analysis was studied, as it causes changes in the flows composition.

System description

For the clinker production, the mix of finely ground raw materials called raw meal passes through heating in order to activate a series of chemical reactions that will result in the main clinker compounds. The major reactions are limestone calcination and the clinkerization reactions given by Eqs. (1–5) (Anacleto et al. 2018; Çamdali et al. 2004).

$$CaCO_3 \rightarrow CaO + CO_2 \tag{1}$$

$$2CaO + SiO_2 \rightarrow (CaO)_2SiO_2 \tag{2}$$

$$CaOAl_2O_3 + 2CaO \rightarrow (CaO)_3Al_2O_3 \tag{3}$$

$$CaOAl_2O_3 + 3CaO + Fe_2O_3 \rightarrow (CaO)_4Al_2O_3Fe_2O_3 \tag{4}$$

$$(CaO)_2SiO_2 + CaO \rightarrow (CaO)_3SiO_2 \tag{5}$$

This process occurs in the pyro processing unit, composed of three sections, as illustrated in Fig. 1. In the preheating section (first section), the raw meal passes through the cyclones-tower and the calciner, when present. In this step, the raw meal is pre-heated by the rotary kiln exhaust gases and goes through most of the calcination. This stage is commonly known as pre-heating or pre-calcination. In the second section, the pre-calcined raw meal, called hot meal, enters the rotary kiln, where the calcination is finished and the clinkerization is carried out. Finally, the clinker is cooled in the cooling section.

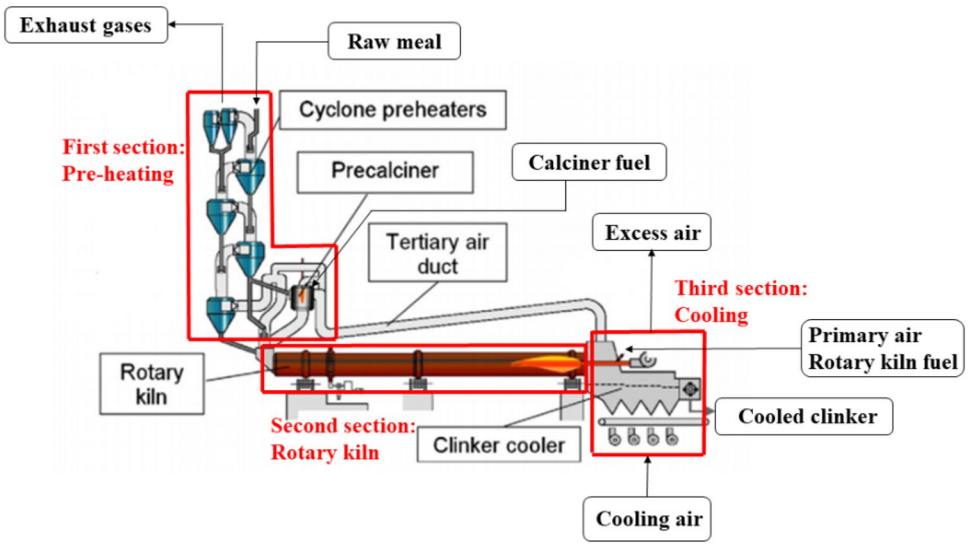

Fig. 1 Example of a pyro processing unit (adapted from Giannopoulos et al. (2007))

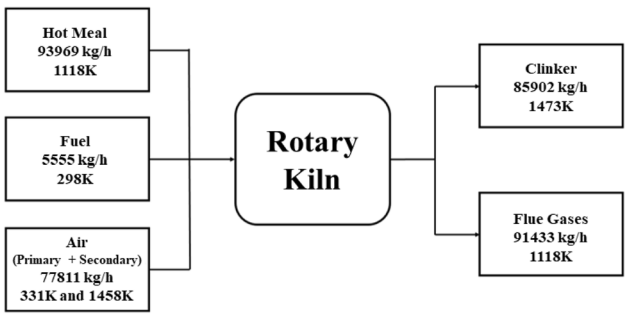

Fig. 2 Control volume—Rotary Kiln

In the present study, a rotary kiln of a Brazilian Cement Plant was considered as the control volume for the energetic and exergetic analysis. The rotary kiln dimensions are 4.1 m of diameter and 62.0 m in length. The rotary kiln inlet flows are the hot meal, fuel and primary and secondary air, while the outlet streams are the clinker and flue gases, as shown in Fig. 2. When the rotary kiln is operating stably, which means that the goal of production are being reached, the following conditions are observed: the secondary air corresponds to 87.18% of the total inlet air, the total inlet air mass flow is in excess in relation to the stoichiometric value to promote complete combustion (5% of flue gases mass flow rate corresponds to oxygen provided by the excess air), the average rotary kiln wall temperature is 168 °C, the hot meal SO_3 mass flow corresponds to 1.18% of the respective total mass flow, hot meal is 83% pre-calcined and it is possible to consider that the fuel ashes aggregate to the clinker. The mass flow and temperatures of the substances in the rotary kiln at a stable operation are given in Table 1. The whole pyro processing unit in this Brazilian Plant presents an average thermal energy consumption of 3684 MJ per ton of clinker.

For a stable operation of the rotary kiln, the following premises can be considered to propose the mass, energy and exergy balances:

(i) Steady state operation.
(ii) Kinetic and potential energy and exergy variation can be neglected.
(iii) There is no change of pressure in the control volume.
(iv) The volume of the control volume is constant.
(v) The electrical work can be neglected.
(vi) Leakage air can be neglected.

Mass analysis (balance and pre-calcination simulation)

The mass conservation equation for an open system operating in a steady state, such as the rotary kiln, is written as Eq. (6).

$$\sum \dot{m}_{in} = \sum \dot{m}_{out} \tag{6}$$

Based on the mass conservation, a simulation was performed to predict how the stream mass flow and composition change as a function of the hot meal percentage of pre-calcination that enters the rotary kiln. This simulation was performed in order to verify the pre-calcination impact in the rotary kiln energy and exergy analyses. Usually cement industries operate with a range of 75–95% of pre-calcination. Then, this was the range explored in the simulation. The starting point for the simulation was the operational conditions showed in Table 1, referent to an operation with 83% of pre-calcination. As mentioned previously, the clinker mass flow and composition, as well as the specific heat consumption of the pyro processing unit are fixed goals of

Table 1 Rotary kiln operational conditions

Inlet		Outlet	
Hot meal (1118 K)	Mass flow rate (kg/h)	Clinker (1473 K)	Mass flow rate (kg/h)
CaO	47,810	C3S	59,474
SiO_2	18,140	C2S	7290
Fe_2O_3	2900	C3A	7829
Al_2O_3	4804	C4AF	8887
Na_2O	136	Na_2O	137
SO_3	1109	SO_3	503
$CaCO_3$	17,355	K_2O	661
K_2O	659	P_2O_5	1121
P_2O_5	1056	Total	85,902
Total	93,969		
Fuel (298 K)	Mass flow rate (kg/h)	Flue gases (1118 K)	Mass flow rate (kg/h)
C	4564	CO_2	24,372
O_2	292	H_2O	1912
N_2	90	N_2	59,844
H_2	200	O_2	4573
S	123	SO_2	732
P_2O_5	65	Total	91,433
Na_2O	2		
K_2O	3		
CaO	25		
Fe_2O_3	20		
Al_2O_3	15		
SiO_2	45		
H_2O	111		
Total	5555		
Air (331 K and 1458 K)	Mass flow rate (kg/h)		
O_2	18,056		
N_2	59,755		
Total	77,811		
Total	177,335	Total	177,335

C3S: $(CaO)_3SiO_2$; C2S: $(CaO)_2SiO_2$; C3A: $(CaO)_3Al_2O_3$; C4AF: $(CaO)_4Al_2O_3Fe_2O_3$

production. Then, these conditions are constant in all simulation scenarios.

Although the pyro processing unit heat consumption is constant, the rotary kiln heat consumption changes for different conditions of pre-calcination. For the equipment under study, when the pre-calcination percentage is lower than 83%, it is necessary to calcine a higher mass of limestone in the kiln than it is necessary in the usual operational conditions, since the hot meal has a higher content of limestone in this condition. Thus, a higher fuel mass flow rate is required in the rotary kiln. From this statement, it is also possible to consider that a lower fuel mass flow is necessary in the calciner in the pre-heating stage, keeping the pyro processing unit heat consumption fixed and respecting the production goals. In the simulation, this increase in the rotary kiln fuel mass flow was calculated using the respective lower heating value (31,342 kJ/kg) and the enthalpy of reaction for the calcination reaction (1781.55 kJ/kg $CaCO_3$). The fuel mass flow increase corresponds to the necessary to promote the extra hot meal calcination. When the pre-calcination percentage is higher than 83%, the opposite situation will occur. Overall, the total flow rate of fuel in the system (kiln and pre-heater) will be kept constant, while the proportion of fuel at each injection point will vary according to the considered pre-calcination rate.

As mentioned previously, in this process all the fuel ash goes to the clinker. Therefore, as the mass flow and composition of the clinker are constant and the fuel mass flow rate in the rotary kiln changes, the hot meal substances mass flow changes in the simulation in order to respect the mass conservation law. Moreover, the mass flow and composition of the flue gases also change in each scenario, since this flow is a function of the fuel, limestone and air mass flow rate. The inlet air mass flow rate in each scenario is in excess in

relation to the stoichiometric value, as mentioned previously. Air mass flow is defined in such a way that 5% of the flue gases mass flow rate corresponds to oxygen.

Thus, except for the clinker, all the process mass flow rates in the simulation change as a function of the percentage of pre-calcination. Moreover, hot meal and flue gas compositions also change. As the variation in the fuel mass flow rate is exactly the value to compensate the variation in the percentage of the calcination reaction that occurs in the rotary kiln, the process reaction enthalpy does not change. However, it is expected that the energetic efficiency will change as a function of the components' enthalpy and the process mass flow rate variation. In addition, it is expected for the chemical exergy contribution in the exergy balance to present a relevant variation in the simulation due to the variation of the mass flow compositions.

In this study, although the rotary kiln flows (except for the clinker flow) change, the whole pyro processing unit balance is kept the same, since the clinker mass flow rate and composition does not change (the same with the pyro processing thermal consumption). Consequently, the change in the rotary kiln balance in this study promotes a change in the pre-heating stage that balances it, in a way that the pyro processing unit does not change.

Data from the simulated scenario of 75% of pre-calcination are given in Table 2 in order to illustrate the methodology. In this scenario, it is possible to observe that, except for the lime, the hot meal substances that are also present in the fuel ash enter the kiln at a lower mass flow rate. This occurs because, as the extra fuel ash will incorporate the material, a lower amount of these substances is necessary to get the desired clinker composition. Lime is an exception because the respective mass is strongly connected to the percentage of pre-calcination. This extra calcination in the rotary kiln also causes extra CO_2 in this equipment's flue gases. Moreover, in this scenario a higher air mass flow rate

Table 2 Rotary kiln simulated conditions for 75% of pre-calcination

Inlet		Outlet	
Hot meal (1118 K)	Mass flow rate (kg/h)	Clinker (1473 K)	Mass flow rate (kg/h)
CaO	43,135	CaO	59,474
SiO_2	18,137	SiO_2	7290
Fe_2O_3	2899	Fe_2O_3	7829
Al_2O_3	4803	Al_2O_3	8887
Na_2O	136	Na_2O	137
SO_3	1152	SO_3	503
$CaCO_3$	25,698	K_2O	661
K_2O	658	P_2O_5	1121
P_2O_5	1051	Total	85,902
Total	97,669		
Fuel (298 K)	Mass flow rate (kg/h)	Flue gases (1300 K)	Mass flow rate (kg/h)
C	4954	CO_2	29,472
O_2	317	H_2O	2075
N_2	97	N_2	65,540
H_2	217	O_2	5152
S	134	SO_2	788
P_2O_5	70	Total	103,027
Na_2O	2		
K_2O	3		
CaO	27		
Fe_2O_3	22		
Al_2O_3	16		
SiO_2	48		
H_2O	121		
Total	6028		
Air (331 K and 1473 K)	Mass flow rate (kg/h)		
O_2	19,789		
N_2	65,443		
Total	85,232		
Total	188,929	Total	188,929

is necessary to allow the complete fuel burn, resulting in a higher flue gas mass flow. SO_3 mass flow in the hot meal is fixed as 1.18% of the total hot meal mass flow. Finally, in this scenario, it is necessary to provide an extra energy flow rate of 14,863,486 kJ/h (compared to the usual operational conditions) to promote the extra calcination inside the rotary kiln, which requires an extra fuel mass flow rate of 473 kg/h in relation to the usual operational conditions.

Energy analysis

The energy balance general equation for a steady state process can be written as Eq. (7) (Caglayan and Caliskan 2018; Gürtürk and Oztop 2014).

$$0 = \dot{Q} - \dot{W} + \sum \dot{m}_{in}\left(h_{in} + \frac{v_{in}^2}{2} + gz_{in}\right) - \sum \dot{m}_{out}\left(h_{out} + \frac{v_{out}^2}{2} + gz_{out}\right) \tag{7}$$

Considering the conditions previously presented in the system description, the energy balance of this process can be written as Eq. (8).

$$\sum \dot{m}_{out} \cdot h_{out} - \sum \dot{m}_{in} \cdot h_{in} = \dot{Q} \tag{8}$$

The specific enthalpy can be calculated using the substances heat capacities and constant pressure, as shown in Eq. (9). Table 3 comprises the parameters for the calculation of the heat capacities at constant pressure for each substance involved in this process (Çamdali et al. 2004).

$$h(T) = h_{f,0} + \int_{T_0}^{T} c_P dT \tag{9}$$

Since the process energy loss corresponds to the rotary kiln heat loss, the energetic efficiency can be described as Eq. (10) (Atmaca and Yumrutas 2014a).

$$\eta_{en} = 1 - \frac{\dot{Q}}{\dot{E}_{in}} \tag{10}$$

Exergy analysis

The exergy can be defined as a system work potential in relation to a reference equilibrium state (Som and Datta 2008). In other words, the exergy represents the maximum work that could be obtained for a system in a transformation in which the system conditions correspond to the initial state and the reference conditions correspond to the final state (Darvishi 2017; Ortega-Delgado et al. 2019; Özilgen 2018). In the exergy analysis the reference state is usually the environment (Bühler et al. 2018). If a system presents the same temperature and pressure of the environment, meaning a thermomechanical equilibrium, the system in considered to be in the "restricted dead state", also denominated by just "environment state". If a system is in a thermomechanical and chemical equilibrium with the environment, it is in the "absolute dead state" (Bühler et al. 2018). In the absolute dead state, no work can be obtained for the system.

In the exergy analysis both the First and the Second Law of Thermodynamics are considered, since the exergy is a thermodynamic property originated from the combination of the two laws (Mastral et al. 2018; Terehovics et al. 2017). Different from the energy, exergy can be destroyed due to the process irreversibilities, associated with the entropy generation (Bühler et al. 2018). Exergy balance for a steady state process can be described as Eq. (11) (Ustaoglu et al. 2017).

$$\sum \dot{m}_{in} ex_{in} - \sum \dot{m}_{out} ex_{out} + \sum \left(1 - \frac{T}{T_0}\right)\dot{Q}_j - \dot{W} = \underset{d}{Ex} \tag{11}$$

In Eq. 11, the first and second terms correspond to the exergy flow, the third represent the exergy loss, related to the heat loss, the fourth term is the exergy related to the work, which is the work itself, and the last term is the exergy destruction, related to the entropy generation and described by Eq. (12) (Costa 2016; Ramos et al. 2019). The temperature considered to calculate the exergy loss in this work was the rotary kiln wall average temperature. Since the kinetic and potential exergies are neglected in this study, the specific flow exergy can be written as Eq. (13) (Bühler et al. 2018).

$$\dot{E}x_d = T_0 \dot{S}_{gen} \tag{12}$$

$$ex = \left[\left(h - h_0\right) - T_0\left(s - s_0\right)\right] + \left[\sum_i \left(\mu_{i,0} - \mu_{i,00}\right)x_i\right] \tag{13}$$

where the terms $h - h_0$ and $s - s_0$ can be calculated by the Eqs. (14) and (15), respectively.

$$h - h_0 = \int_{T_0}^{T} c_P dT \tag{14}$$

$$s - s_0 = \int_{T_0}^{T} \frac{c_P}{T} dT \tag{15}$$

The first term in Eq. (13) represents the physical exergy contribution, while the second term describes the chemical

Table 3 Parameters for the calculation of the substances heat capacities at constant pressure

Substance	α	β	σ	δ	ε	T (K)
$CaO^{1,a}$	49.95403	4.887916	− 0.352056	0.046187	− 0.825097	298–3200
$SiO_2{}^{1,a}$	72.77482	1.293543	− 0.004360	0.000798	− 4.140645	298–1996
$Fe_2O_3{}^{1,a}$	93.43834	108.3577	− 50.86447	25.58683	− 1.611330	298–950
	150.624	–	–		–	950–1050
	110.9362	32.04714	− 9.192333	0.901506	5.433677	1050–2500
$Al_2O_3{}^{1,a}$	102.429	38.7498	− 15.91090	2.628181	− 3.007551	298–2327
$Na_2O^{1,a}$	25.5754	177.71	− 166.3350	57.6116	0.338149	298–1023
	− 125.7730	302.074	− 140.6420	21.324	38.2831	1023–1243
$SO_3{}^{1,a}$	24.02503	119.4607	− 94.38686	26.96237	− 0.117517	298–1200
$CaCO_3{}^{2,b}$	12.572	2.637×10^{-3}	-3.120×10^{5}	–	–	298–1200
$K_2O^{1,a}$	245.0104	− 567.0492	778.7219	− 346.2641	− 4.653361	298–700
	72.55098	41.39097	− 0.728497	0.218564	0.066026	700–2000
$P_2O_5{}^{3,c}$	− 21.643407	0.3362284	-3.516373×10^{6}	1.126290×10^{-4}	2.2900402×10^{4}	298–1000
	225.000000	–	–	–	–	> 1000
$C^{2,b}$	1.771	0.771×10^{-3}	-0.867×10^{5}	–	–	298–2000
$S^{1,a}$	21.21978	3.865858	22.27461	− 10.31908	− 0.122518	298–388,36
$N_2{}^{1,a}$	28.98641	1.853978	− 9.647459	16.63537	0.000117	100–500
	19.50583	19.88705	− 8.598535	1.369784	0.527601	500–2000
$H_2{}^{1,a}$	33.066178	− 11.363417	11.432816	− 2.772874	− 0.158558	298–1000
$O_2{}^{1,a}$	31.32234	− 20.23531	57.86644	− 36.50624	− 0.007374	100–700
	30.03235	8.772972	− 3.988133	0.788313	− 0.741599	700–2000
$H_2O^{2,b}$	3.47	1.450×10^{-3}	0.121×10^{5}	–	–	298–2000
$CO_2{}^{1,a}$	24.99735	55.18696	− 33.69137	7.948387	− 0.136638	298–1200
	58.16639	2.720074	− 0.492289	0.038844	− 6.447293	1200–6000
$SO_2{}^{1,a}$	21.43049	74.35094	− 57.75217	16.35534	0.086731	298–1200
	57.48188	1.009328	− 0.076290	0.005174	− 4.045401	1200–6000
$C3S^{4,d-e}$	209	0.036	-4.25×10^{6}	–	–	–
$C2S^{4,d-e}$	152	0.037	-3.03×10^{6}	–	–	–
$C3A^{4,d-e}$	261	0.019	-5.06×10^{6}	–	–	–
$C4AF^{4,d-e}$	374	0.073	–	–	–	–

[a]National Institute of Standard Technology (NIST)

[b]Smith et al. (2007)

[c]Jung and Hudon (2012)

[d]Matschei et al. (2007)

[e]Lothenbach et al. (2019)

[1] $cp(T) = \alpha + \beta\left(\frac{T}{1000}\right) + \sigma\left(\frac{T}{1000}\right)^{2} + \delta\left(\frac{T}{1000}\right)^{3} + \varepsilon\left(\frac{T}{1000}\right)^{-2}$

[2] $cp(T) = R\left(\alpha + \beta T + \sigma T^{-2}\right)$

[3] $cp(T) = \alpha + \beta T + \sigma T^{-2} + \delta T^{2} + \varepsilon T^{-1}$

[4] $cp(T) = \alpha + \beta T + \sigma T^{-2} + \delta T^{-0.5}$

exergy contribution, defined as ex^{0}_{ch}. The physical exergy corresponds to the energy available to produce work when the flow is brought from its state to the "restricted dead state". On the other hand, the chemical exergy corresponds to the energy available when the flow is brought from the "restricted dead state" conditions to the "absolute dead state" (Araújo et al. 2007). Most of the literature describes the "restricted dead state" as the standard ambient conditions (Anacleto et al. 2018; Bühler et al. 2018; Fellaou et al. 2018; Ustaoglu et al. 2017; Yildirim and Genc 2017). However, to describe the absolute dead state it is also necessary to define the reference state composition. Substance chemical exergy can be calculated based on three reference states: atmospheric gaseous composition, sea water composition and lithosphere composition (Szargut 1989). The more abundant species in each of these states are taken as references species. Chemical exergy calculation is different for each

reference state. Gaseous reference species in the atmosphere standard chemical exergy are defined by Eq. (16) (Ustaoglu et al. 2017).

$$ex_{ch}^{0} = RT_0 \ln\left(\frac{P_{i,0}}{P_{i,00}}\right) \tag{16}$$

Standard chemical exergy for solid reference species in the litosphere is given by Eq. (17) (Szargut 1989).

$$ex_{ch}^{0} = -RT_0 \ln(\chi_i) \tag{17}$$

where χ_i is corresponds to the reference specie mole fraction in the lithosphere, calculated by Eq. (18) (Szargut 1989).

$$\chi_i = \frac{n_{i,0} c_i M_0}{l_i} \tag{18}$$

Standard chemical exergy for an element for which the reference specie is dissolved in sea water can be calculated by Eq. (19), where the pH is considered to be 8.1 (Szargut 1989).

$$ex_{ch}^{0} = j\left[-\Delta g_f^0 + \frac{1}{2} Z ex_{ch,H_2}^{0} - \sum_k N_k ex_{ch,k}^{0} - 2.303 RT_0 Z(pH) - RT_0 \ln\left(u_0 \gamma\right)\right] \tag{19}$$

Elemental standard chemical exergies are used to calculate non-reference substance chemical exergies. In order to calculate these non-reference substance chemical exergies, it is required to propose their formation reactions by using only reference species as reactants. This allows calculating the substance chemical exergy using Eq. (20) (Gharagheizi et al. 2014; Rivero and Garfias 2006; Song et al. 2012; Szargut 1989).

$$ex_{ch}^{0} = \Delta g_f^0 + \sum_{el} \nu_{el} ex_{ch,el}^{0} \tag{20}$$

Some studies determined several substance chemical exergies considering these reference states and using these reference species. This data was used to develop the exergy balance in this work (Qian et al. 2017; Rivero and Garfias 2006; Song et al. 2012; Szargut 1989). Moreover, based on Eq. 20 and using data from substances for which the standard chemical exergy was already calculated, it is possible to determine other substance chemical exergies by a proposition of chemical reactions in which only the standard chemical exergy of the substance of interest is unknown applying Eq. (21). Clinker component standard chemical exergies used in this work were calculated applying Eq. (21) for the reactions given by Eqs. (2), (3), (4) and (5). Clinker component standard chemical exergies calculated directly from Eq. (20) and calculated by Eq. (21) can be seen in the appendix. Fuel standard chemical exergy on a dry basis can be estimated by Eq. (22), developed by Song et al. (2012).

$$ex_{ch}^{0} = \Delta g_r^0 + \sum_i \nu_i ex_{ch,i}^{0}. \tag{21}$$

$$ex_{ch,coal}^{0} = 363.439C + 1075.633H - 86.308O + 4.147N + 190.798S - 21.1A(\text{kJ/kg}) \tag{22}$$

Gaseous streams chemical exergy, such as the flue gases, are calculated using the substance standard chemical exergy in Eq. (23) (Querino et al. 2019).

$$ex_{ch}^{0} = \sum_i x_i ex_{ch,i}^{0} + RT_0 \sum_i x_i \ln(x_i) \tag{23}$$

As mentioned previously, there are classical and modern approaches in the exergetic efficiency calculation. The classical exergetic efficiency can be defined by Eq. (24), in order to evaluate how effectively the input exergy is conserved in the process (Çamdali et al. 2004; Ustaoglu et al. 2017).

$$\eta_{ex} = \frac{Ex_{out}}{Ex_{in}} \tag{24}$$

Modern exergetic efficiency can be defined by Eq. (25) and allows quantifying how effectively the fuel exergy is converted into the desired product exergy (Lazzaretto and Tsatsaronis 2006; Madlool et al. 2012; Vučković et al. 2014).

$$\eta_{ex} = \frac{Ex_P}{Ex_F} \tag{25}$$

The concept of fuel in the modern exergetic efficiency analysis is not restricted to the fuel consumed in the process. According to Lazzaretto and Tsatsaronis (2006) the fuel corresponds to all the resources expended in order to produce the desired product. Thus, exergetic efficiency can also be represented by Eq. (26) (Madlool et al. 2012).

$$\eta_{ex} = \frac{\textit{Desired exergetic effect}}{\textit{Exergy used to drive the process}} = \frac{Ex_P}{Ex_F} \tag{26}$$

In the present study, the desired product is the clinker, while the fuel used to drive the process corresponds to the contribution of all the inlet streams (hot meal, fuel and air). In this context, flue gas exergy is a loss (undesired).

Moreover, the authors applied the concept of modern exergetic efficiency to the energetic efficiency calculation. In this approach, energetic efficiency can be calculated by Eq. (27).

$$\eta_{en} = \frac{\dot{E}_P}{\dot{E}_F} = \frac{Desiredenergeticeffect}{Energyusedtodrivetheprocess} \quad (27)$$

Methodology

The methodology adopted in this study consists mainly of the process description using mass balance and thermodynamic tools. The major aspects used in the energy and exergy analysis were previously presented. The diagram shown in Fig. 3 illustrates the methodology used. Pre-calcination analysis was developed adopting the methodology which considers all the system chemical exergy, in order to detect the chemical exergy impact in the exergy analysis related to the flows change of composition.

Results and discussion

Energy analysis

Energetic analysis of this process using data from Table 1 resulted in a classical energetic efficiency of 63.9%. This value is not distant from the value obtained by Atmaca and

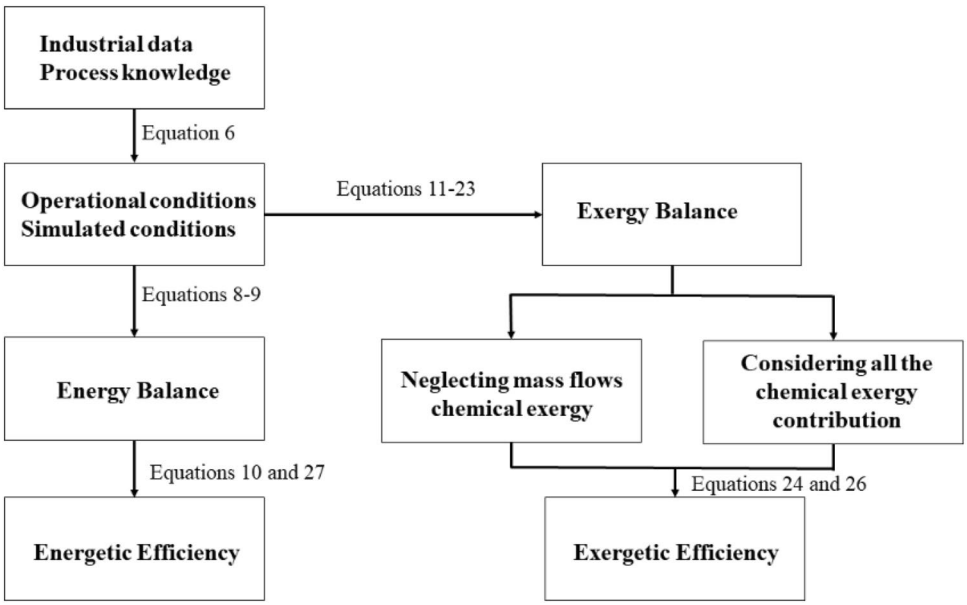

Fig. 3 Methodology schematic diagram

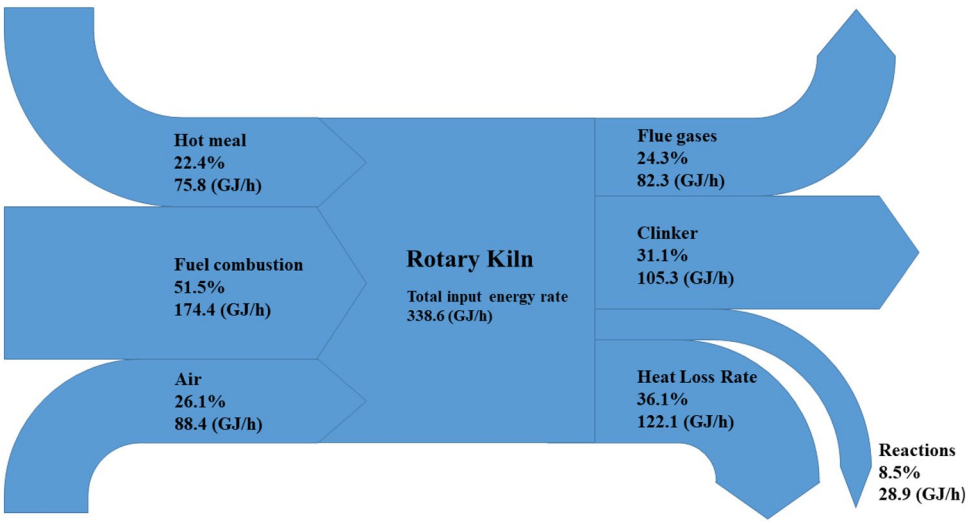

Fig. 4 Process Sankey diagram

Table 4 Rotary Kiln energy balance

	$\dot{m}$(kg/h)	T_0(K)	T (K)	$\dot{m}\Delta h$(kJ/h)	Percentage (%)
Inlet					
Hot meal	93,969	298	1118	75,851,606	22,4%
Fuel	5555	298	298	0	0,0%
Primary air	9974	298	331	334,519	0,1%
Secondary air	67,837	298	1458	88,027,273	26,0%
Fuel combustion	–	–	–	174,385,211	51,5%
Total	177,335			338,598,609	100,0%
Outlet					
Clinker	85,902	298	1473	105,324,183	31,1%
Flue Gases	91,433	298	1118	82,264,947	24,3%
Reactions	–	–	–	28,860,160	8,5%
Heat loss	–	–	–	122,149,319	36,1%
Total	177,335			338,598,609	100,0%

Yumrutas, (2014a) (55.8%). The rotary kiln heat loss rate is approximately 1.2×10^{8} kJ.hr^{-1}. The rotary kiln energy balance can be seen in Table 4 and Fig. 4.

The results presented in Table 5 allow deducing that the major energy contribution to the rotary kiln comes from the fuel combustion as expected. However, the secondary air energy contribution to the process is also relevant. This result confirms the benefit of the use of the secondary air (obtained from the clinker cooler outlet air) as an input of the system with the aim of recovering energy. Moreover, the rotary kiln exhaust gases carry out a considerable part of the rotary kiln inlet energy. Therefore, efforts in order to recover this available energy in other process units are justifiable. Modern cement plants usually recover rotary kiln exhaust gases energy, using them for drying the raw meal and fuel in the grinding processes. Flue gases can also be used in Organic Rankine Cycles for power generation (Ustaoglu et al. 2017).

Although it is possible to recover the flue gas energy, in the modern efficiency analysis this stream energy can be considered a loss. In this process, the desire is to convert the inlet energy into the desired product, maximizing the desired product energy. Since the flue gases consume a fraction of the energy that should be transferred to the clinker, flue gas energy is undesired and must be minimized. Taking into consideration this approach, the rotary kiln modern energetic efficiency is 31.1%, calculated by Eq. (27).

Exergy analysis

The exergy balance was developed using the data from Table 1. Data for the exergy balance performed neglecting the stream chemical exergy can be seen in Table 5, while the data corresponding to the complete exergy balance are exposed in Table 6.

The exergetic efficiency obtained using Eq. 21 and data from Table 5 corresponds to 38.2%. This value is close to the value obtained by Atmaca and Yumrutas (2014) (38.7%), who adopted the same methodology applied to generate Table 5 data. This result indicates that the rotary kiln data used in this study are reliable. The exergy balance is illustrated in the Grassmann Diagram shown in Fig. 5.

Modern exergetic efficiency calculated by Eq. 26 and data from Table 5 corresponds to 22.6%. This value is inferior to that obtained by the classical evaluation, which is justifiable, since in this case flue gas exergy does not contribute to the exergetic efficiency. Modern exergetic efficiency for the rotary kilns studied by Çamdali et al. (2004) and Atmaca and Yumrutas (2014) are 18.8% and 16.7%, respectively. These rotary kilns present a lower efficiency value than that obtained in the present work

Table 5 Rotary kiln exergy balance neglecting streams chemical exergy

	Physical Exergy Rate (kJ/h)	Chemical Exergy Rate (kJ/h)	Total exergy Rate (kJ/h)	Contribution to the total exergy (%)
Inlet				
Hot meal	40,787,530	0	40,787,530	14.5%
Fuel	0	187,259,154	187,259,154	66.6%
Air	53,080,724	0	53,080,724	18.9%
Total	93,868,254	187,259,154	281,127,408	100.0%
Outlet				
Clinker	63,668,780	0	63,668,780	22.6%
Flue gases	43,658,262	0	43,658,262	15.6%
Parcial total	107,327,042	0	107,327,042	38.2%
Exergy lost			39,636,575	14.1%
Exergy destroyed			134,163,791	47.7%

Table 6 Rotary kiln complete exergy balance

	Physical exergy rate (kJ/h)	Chemical exergy rate (kJ/h)	Total exergy rate (kJ/h)	Physical exergy percentage	Chemical exergy percentage
Inlet					
Hot meal	40,787,530	124,784,423	165,571,953	24.6%	75.4%
Fuel	0	187,259,154	187,259,154	0.0%	100.0%
Air	53,080,724	0	53,080,724	100.0%	0.0%
Total	93,868,254	312,043,577	405,911,831	23.1%	76.9%
Outlet					
Clinker	63,668,780	106,124,606	169,793,386	37.5%	62.5%
Flue gases	43,658,262	11,753,573	55,411,835	78.8%	21.2%
Parcial total	107,327,042	117,878,179	225,205,221	47.7%	52.3%
Exergy lost			39,636,575		
Exergy destroyed			141,070,035		

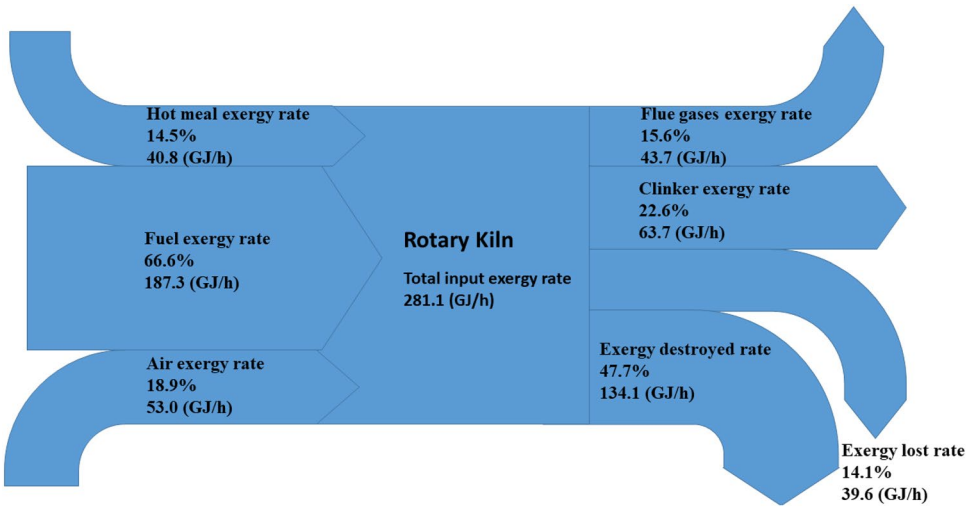

Fig. 5 Process Grassmann diagram (neglecting stream chemical exergy, except from the fuel)

considering the modern analysis. However, both kilns have a higher efficiency than that obtained in the present work considering the classical analysis. This behavior occurs because flue gas exergy in these rotary kilns had a higher impact in the outlet exergy than in the rotary kiln studied in the present work. Thus, considering the conversion of the inlet exergy into the desired product, the rotary kiln studied in the present work is the most efficient among these three studied ones.

On the other hand, values obtained in Table 6 allow inferring that the chemical exergy presents a relevant contribution to the total exergy of this process. This result indicates that, even in the exergetic analysis of systems that involve flows with high temperature, the chemical exergy contribution cannot be neglected. The chemical exergy presented the highest impacts in the exergy evaluation from the hot meal, fuel and clinker. The contribution of the chemical exergy in the total exergy of the flue gases showed a lower relevance. This occurred because the substances in these solid flows have a higher potential to perform work due to the higher chemical potential difference between their current state and the absolute dead state condition. The complete exergy balance is illustrated in the Grassmann Diagram exposed in Fig. 6.

In this methodology, the rotary kiln classical exergetic efficiency was 55.5%. If Çamdali et al. (2004) and Atmaca and Yumrutas (2014) had considered flow chemical exergy, the classical exergetic efficiency from their rotary kilns would be 76.7% and 45.8%, respectively. In all the cases, the efficiency is considerably different from that calculated neglecting the stream chemical exergy, which indicates that stream chemical exergy is relevant in any clinker rotary kiln analysis.

The rotary kiln modern exergetic efficiency considering Table 6 data and applying Eq. (26) is 41.8%. This analysis for the studies of Çamdali et al. (2004) and Atmaca and Yumrutas (2014) results in an efficiency of 34.6% and 26.8%. In both methodologies (considering and neglecting the streams chemical exergy), it can be observed that the

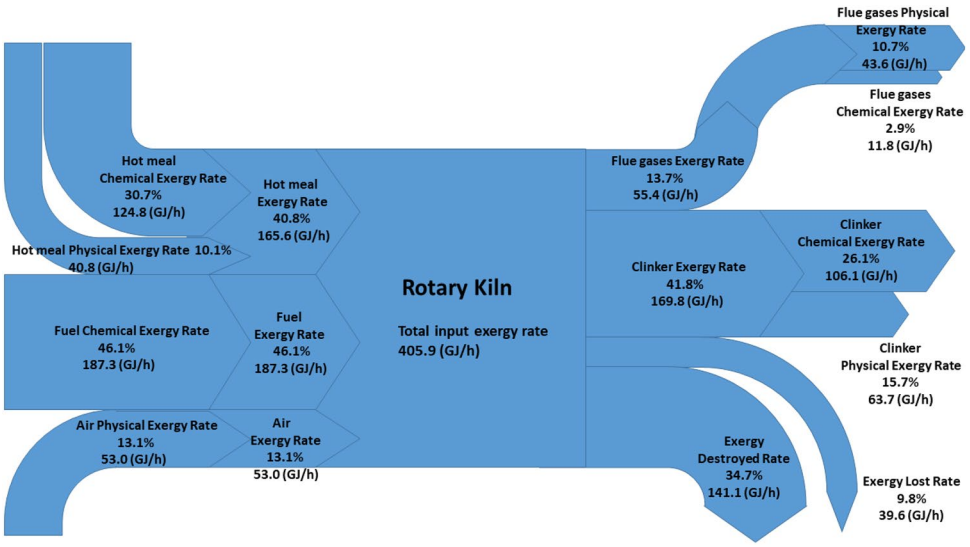

Fig. 6 Process Grassmann diagram

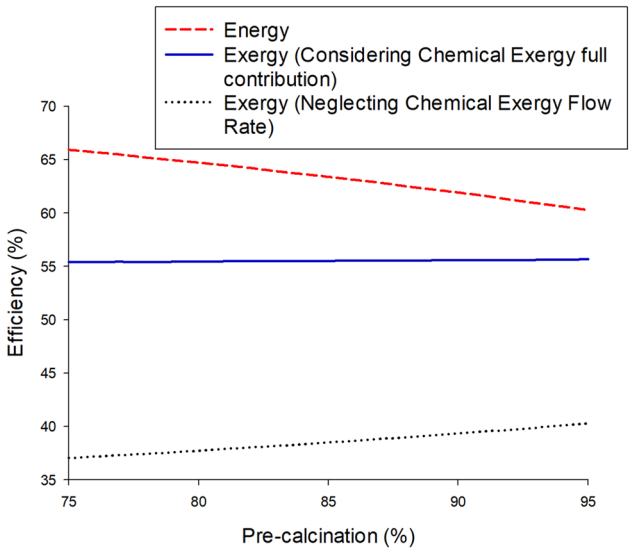

Fig. 7 Pre-calcination effect on the classical energetic and exergetic efficiency

concept employed in the efficiency analysis leads to different interpretations. While classical exergetic efficiency points to the rotary kiln studied by Çamdali et al. (2004) as the most efficient, modern exergetic efficiency points to the rotary kiln studied in the present work as the most efficient one. Thus, it is important to evaluate carefully which concept of efficiency can be more realistic for the process in consideration, since different concepts of efficiency can lead to different interpretations of the system under study.

Pre-calcination analysis

The pre-calcination influence on the classical energetic and exergetic efficiencies is shown in Fig. 7. From Fig. 7 it can be seen that the rotary kiln energetic efficiency reduces with the percentage of pre-calcination increase. The energy demand variation is due to the percentage of pre-calcination and this is balanced by the fuel mass flow rate in the simulation, as mentioned previously. However, the pre-calcination also affects the hot meal and flue gas enthalpies due to their composition variation, especially the change in the limestone and lime ratio in the hot meal and in the CO_2 mass rate change in the flue gases. The increase in the pre-calcination caused a reduction in the hot meal, air and flue gas enthalpies, but the reduction in the flue gas enthalpy was more relevant.

Since the pyro processing unit specific heat consumption was kept constant (as well as the composition and mass rate of the clinker), this reduction in the rotary kiln classical energetic efficiency causes an increase in the pre-heating stage efficiency. Therefore, this result does not allow concluding that the pre-calcination is not indicated. Usually in a real process the increase in the percentage of pre-calcination causes a reduction in the pyro processing unit specific heat consumption, which would balance the observed classical energetic efficiency reduction in this simulation.

The classical exergetic efficiency when the flow chemical exergy was neglected shows that the rotary kiln efficiency clearly increases when the percentage of pre-calcination is higher. This result is different from that observed when all the chemical exergy is considered, which means that the methodology adopted in the exergy analysis can influence even the system interpretation. Thus, it is inadequate to disregard the flow chemical exergy in the rotary kiln exergy analysis.

When all the chemical exergy contributions are considered, the classical exergetic efficiency was not considerably affected by the percentage of pre-calcination. Just a slightly increase in the efficiency proportional to the percentage of

pre-calcination can be seen, inferior to 1%. This occurred because its effect on the hot meal exergy balanced the effect on the fuel combustion exergy. In addition, the output exergy did not change considerably in the simulation.

The pre-calcination influence on the modern energetic and exergetic efficiencies is shown in Fig. 8. Different from that observed in the classical analysis, in this modern approach, the rotary kiln energetic and exergetic efficiencies increase when the percentage of pre-calcination increases. This result is more realistic for the process than the results obtained by the classical analysis. The higher the percentage of pre-calcination, the lower is the fuel mass flow rate required in the rotary kiln, as it is necessary to promote a lower percentage of the calcination reaction inside the equipment, which is an endothermic reaction. Thus, it is expected that the rotary kiln efficiency increases with the increase of the pre-calcination, as observed in the modern analysis. Furthermore, from Fig. 8 it is possible to observe that, although all the curves presented a similar behavior in the modern efficiency analysis, when the stream chemical exergy contribution was considered in the analysis, efficiency values are considerably different from the values when the respective contribution was neglected.

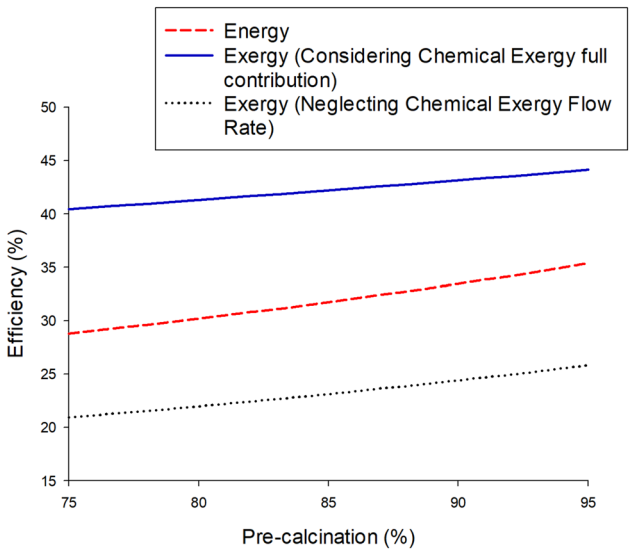

Fig. 8 Pre-calcination effect on the modern energetic and exergetic efficiency

This difference between the results obtained by the classical and modern calculation occurs because, while the first analysis take into account the flue gas energy and exergy contribution in the outlet, the second analysis does not consider flue gas energy and exergy as a useful contribution, disregarding the respective contribution in the efficiency. Since the clinker energy and exergy do not change in the simulation, and the flue gas energy and exergy reduce with the increase of pre-calcination (as will be discussed following), this flue gas behavior causes a reduction in the classical efficiency, reflected in the calculated value. In the modern analysis, since flue gas energy and exergy are not taken into account (undesired energy and exergy), the efficiency variation is related just to the fuel energy and exergy contribution. Therefore, it can be seen that, for a higher percentage of pre-calcination, it is possible to produce the same clinker with a lower fuel energy and exergy consumption.

Pre-calcination and chemical exergy effects in each rotary kiln stream are presented in the following results (physical and chemical exergies of each stream were considered). In these results, it was considered as exergy lost the exergy related to the heat loss and considered as exergy destroyed the exergy related to the irreversibilites (classical concept).

The pre-calcination effect in each input and output of energy and exergy is shown in Figs. 9 and 10. From Fig. 9a it is possible to observe that the fuel combustion and air

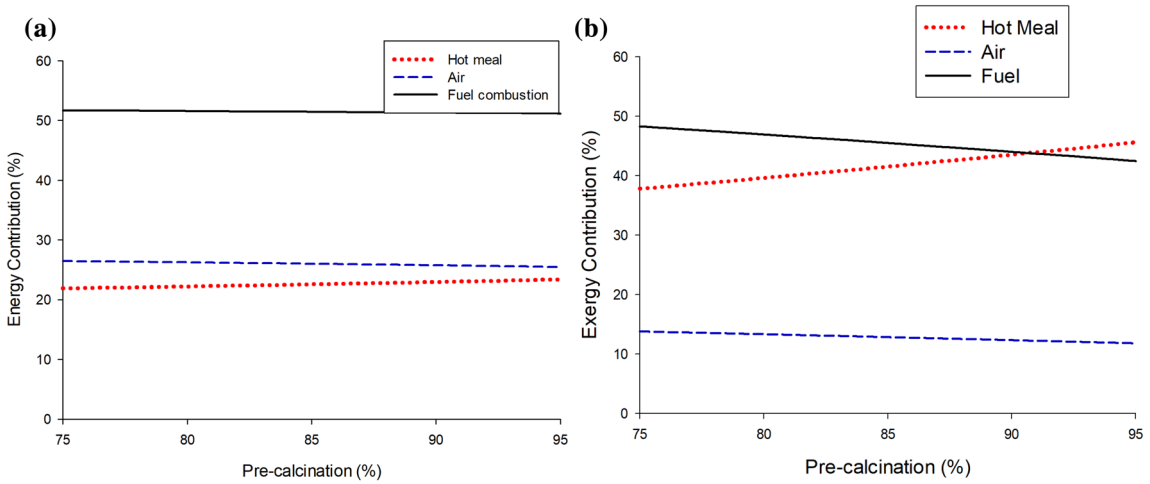

Fig. 9 **a** Effect of pre-calcination on the input energy. **b** Effect of pre-calcination on the input exergy

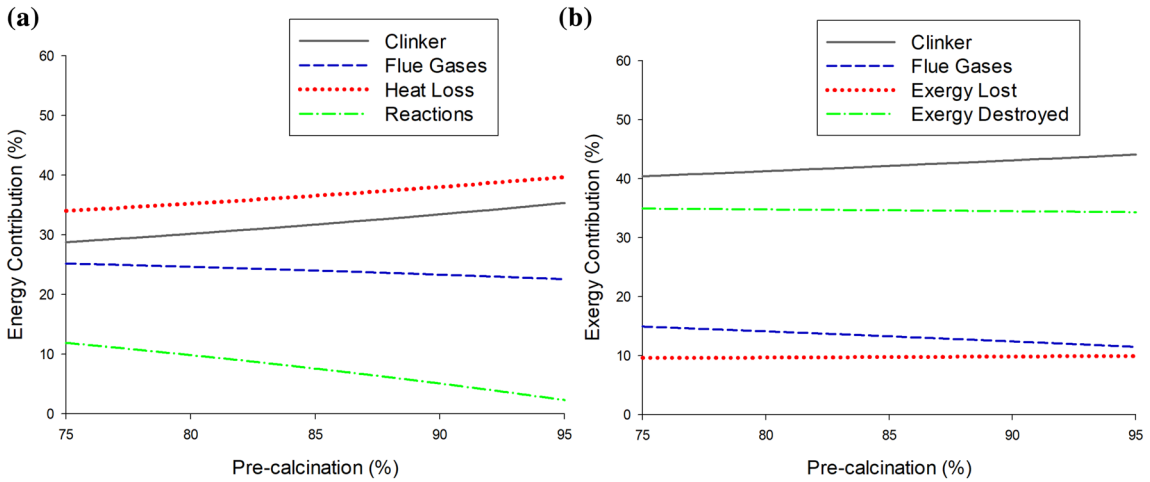

Fig. 10 **a** Effect of pre-calcination on the output energy. **b** Effect of pre-calcination on the output exergy

contributions to the input energy reduced with the increase of the pre-calcination percentage. This is a consequence of the fuel and air mass flow rate reduction associated with the higher pre-calcination. Thus, the hot meal contribution to the inlet energy was higher. The same behavior was observed in the input exergy analysis, but on a larger scale (Fig. 9b). That happened because, in the exergetic analysis, the increase in the pre-calcination causes two effects: a fuel and air exergy contribution reduction due to the decrease of fuel and air mass flow rates, and a hot meal exergy contribution increase, as a consequence of the higher lime mass ratio.

Output flows analysis, illustrated by Figs. 10a, b, shows that the flue gases and clinker had a similar behavior as a function of the percentage of pre-calcination. In this simulation, clinker energy and exergy values are constant, because the mass flow and composition were kept constant. However, its contribution to the outlet energy and exergy increased with the increase of the pre-calcination rate due to the reduction of the flue gases contribution. Flue gas energy and exergy contributions are inversely proportional to the percentage of pre-calcination, because the higher pre-calcination leads to a lower CO_2 mass rate in the flue gases, which results in lower energy and exergy. Since the heat loss is proportional to the percentage of pre-calcination, the exergy loss is also proportional. Finally, the exergy destruction is not affected by the pre-calcination, since the total input and output exergies did not change considerably.

The pre-calcination effect on the chemical exergy analysis is relevant in the hot meal and flue gases. The chemical exergy contribution to the total exergy in these flows changes considerably with the variation in the percentage of pre-calcination, as can be seen in Fig. 11. This change occurs because of the change in the flow composition. The higher the pre-calcination of the hot meal, the higher the CaO ratio in its composition. Since the standard chemical exergy of CaO is higher than the standard chemical

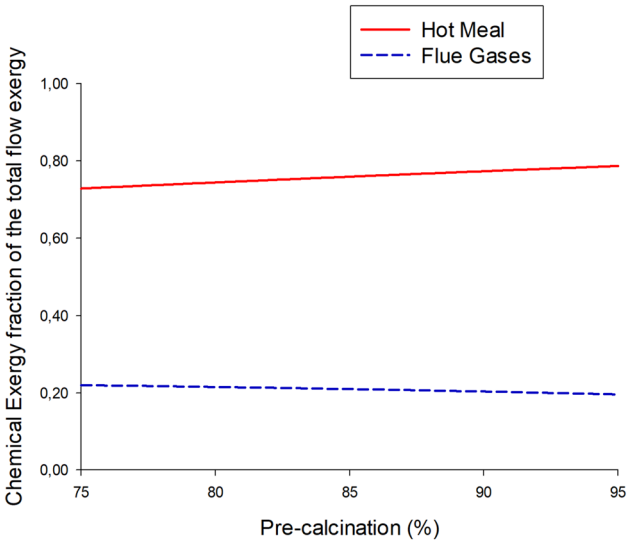

Fig. 11 Flue gases and hot meal chemical exergy fraction as a function of the pre-calcination

exergy of $CaCO_3$, the hot meal chemical exergy increases with an increase in the pre-calcination. Moreover, the higher CaO ratio in hot meal promotes a physical exergy reduction. However, the change of physical exergy in this case is less relevant than the chemical exergy change, as can be seen in Fig. 12. Thus, the higher the pre-calcination, the higher the chemical exergy contribution in the hot meal total exergy. For the flue gases composition, the higher the pre-calcination, the lower the CO_2 ratio. This decrease in the CO_2 ratio results in a reduction of the chemical and physical exergies. However, the chemical exergy reduction is more relevant, as shown in Fig. 13. Thus, the chemical exergy contribution to the hot meal total exergy is directly proportional to the pre-calcination, while the chemical exergy contribution to the flue gas total exergy is inversely proportional to the pre-calcination.

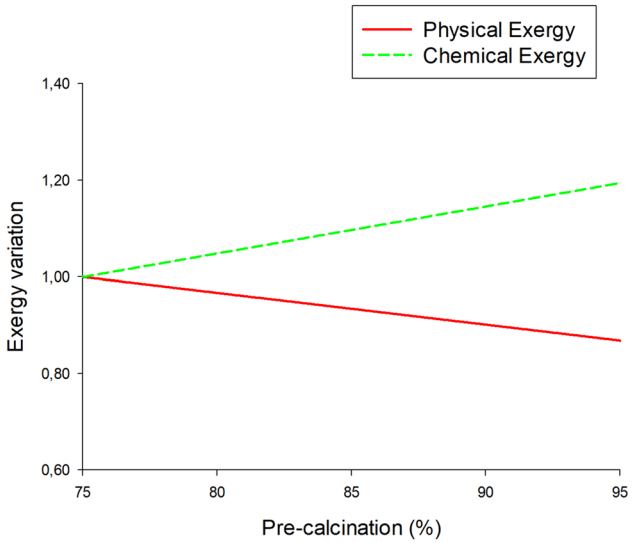

Fig. 12 Hot meal exergy variation as a function of the pre-calcination

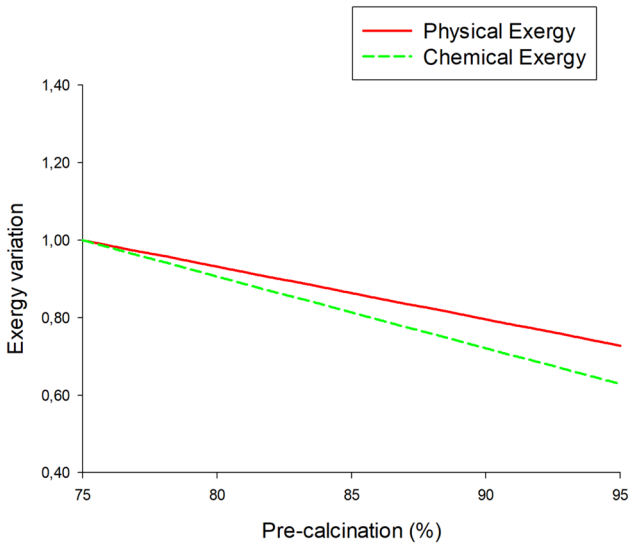

Fig. 13 Flue gases exergy variation as a function of the pre-calcination

Conclusions

In this work an energetic and exergetic analysis of a rotary kiln used for clinker production in a Brazilian Cement plant was performed. The aim of the work was to study the chemical exergy impact on the rotary kiln exergy analysis, also considering the influence of the percentage of pre-calcination. First, the analysis was developed for the usual operational conditions. Posteriorly, the pre-calcination effect on the process was studied.

The rotary kiln classical energy efficiency was 63.9%, not distant for the value obtained by Atmaca and Yumrutas (2014a). Rotary kiln exergy classical efficiency, when considered all the chemical exergy contribution, was 55.5%, while the classical exergy efficiency considering just the fuel chemical exergy was 38.2%. The results indicates that, even in a system with high temperature, such as the rotary kiln, the chemical exergy may be considered in the exergy analysis. In addition, for the both approaches, classical exergetic efficiency was inferior to the classical energetic efficiency calculated following the common literature results. This indicates that exergy analysis really is able to detect system irreversibilities and reinforces its importance in system thermodynamic evaluations.

Considering the modern concept of efficiency, the rotary kiln energy efficiency was 31.1%, significantly inferior to that obtained in the classical analysis. Exergy efficiency when the stream chemical exergy was considered and when the respective contribution was neglected were 41.8% and 22.6%, respectively. Both values are also inferior to those the obtained in the classical analysis. This result indicates that flue gases carried out of the rotary kiln a relevant fraction of the inlet energy and exergy. Flue gas energy and exergy are not used in the rotary kiln and consist in a loss. Efforts in order to recover this loss are justifiable in order to increase the cement plant efficiency.

In relation to the pre-calcination simulation, although the simulation was performed in a way that the pyro processing unit energetic efficiency did not change, the rotary kiln energy and exergy efficiencies changed with the variation of the percentage of pre-calcination. Results showed that the modern concept of efficiency allows performing a more realistic evaluation for the rotary kiln. Considering modern energy and exergy efficiency analysis, it is indicated to operate the rotary kiln using the maximum pre-calcination feasible, since the energy and exergy losses are minimized in this condition. In relation to the irreversibilites, classical exergy analysis showed that the rotary kiln exergy destroyed (by irreversibilities) does not change considerably when the percentage of pre-calcination changes. Usually, irreversibilites are also related to equipment technological limitations. Consequently, in this process, efforts to acquire well designed equipment might be more efficient to reduce process irreversibilities than change some operational conditions.

Rotary kiln energetic and exergetic analysis showed that the pre-calcination effect on the stream energy and exergy contribution to the process followed the same behavior, but the effect on the exergy is more perceptible. This occurred because the substance chemical exergy amplified the pre-calcination influence on the process. Moreover, the stream composition variation as a function of the percentage of pre-calcination showed that the solid stream chemical exergy is more influenced by the composition than the gaseous streams.

All the information necessary to reproduce the obtained results is presented in this article. Thus, it becomes possible to

adapt the proposed methodology to other similar systems and to compare the efficiencies of different clinker rotary kilns.

Acknowledgements The authors are grateful to CNPq—Conselho Nacional de Desenvolvimento Científico e Tecnológico, Capes—Coordenação de Aperfeiçoamento de Pessoal de Nível Superior and FAPEMIG—Fundação de Amparo à Pesquisa do Estado de Minas Gerais (TEC-APQ-00914-16) for the financial support.

Appendix

See Tables 7, 8 and 9

Table 7 Thermodynamics properties standard values

Substance	$h°_f$ (J/mol)	g_f^0(J/mol)	$ex_{ch}°$ (J/mol)
CaO	− 635090[a]	− 1128500[b]	129880[b]
SiO2	− 905490[a]	− 856444[b]	1780[b]
Fe_2O_3	− 825500[a]	− 742294[b]	15550[b]
Al_2O_3	− 1675690[a]	− 1582271[b]	4450[b]
Na_2O	− 417980[a]	− 379090[b]	296320[b]
SO_3	− 395770[a]	− 371017[b]	242000[b]
CaCO3**	− 1207000[c]	− 1128500[b]	19120[b]
K2O	− 363170[a]	− 322766[b]	412540[b]
P2O5	− 1504970[d]	− 1355675[b]	377120[b]
C	0	0	410270[e]
S	0	0	609300[e]
N_2	0	0	670[e]
H_2	0	0	236120[e]
O_2	0	0	3920[e]
H_2O	− 285830[a]	− 237200[c]	9490[f]
CO2	− 393520[a]	− 394380[e]	19870[g]
SO2	− 296840[a]	− 300194[h]	310930[g]
C3S	− 2931000[c,i]	− 2784300[c,i]	273,951*
C2S	− 2308000[c,i]	− 2193200[c,i]	132,052*
C3A	− 3561000[c,i]	− 3382300[c,i]	412,768*
C4AF	− 5080000[c,i]	− 4786500[c,i]	488,781*

[a]National Institute of Standard Technology (NIST)
[b]Song et al. (2012)
[c]Matschei et al. (2007)
[d]Jung and Hudon (2012)
[e]Rivero and Garfias (2006)
[f]Szargut (1989)
[g]Qian et al. (2017)
[h]Smith et al. (2007)
[i]Lothenbach et al. (2019)
*Calculated by Eq. 21
**Calcite

Table 8 Clinker substances chemical exergy

	Chemical exergy calculated by Eq. 21 (J/mol)	Chemical exergy calculated by Eq. 20 (J/mol)
C3S	273,951	267,800
C2S	132,052	127,830
C3A	412,768	404,618
C4AF	488,781	489,500

Table 9 Reactions enthalpies

	Value	Unit
C3S formation (Eq. 5)	13,390	(J/mol)
C2S formation (Eq. 2)	− 126,460	(J/mol)
C3A formation (Eq. 3)	8580	(J/mol)
C4AF formation (Eq. 4)	− 35,140	(J/mol)
Calcination Eq. 1)	178,310	(J/mol)
Fuel low heating value	31,341,891	(J/kg)

References

Anacleto TF, Turetta LF, Jr C, EF; Costa, AOS, (2018) Efeito da reação de calcinação nas análises energética e exergética de um forno rotativo empregado na produção de clínquer. Cerâmica 64:507–518. https://doi.org/10.1590/0366-69132018643722416

Araújo ACB, Vasconcelos LGS, Fossy MF, Brito RP (2007) Exergetic and economic analysis of an industrial distillation column. Braz J Chem Eng 24:461–469. https://doi.org/10.1590/S0104-66322007000300015

Atmaca A, Yumrutas R (2014) Analysis of the parameters affecting energy consumption of a rotary kiln in cement industry. Appl Therm Eng 64:435–444. https://doi.org/10.1016/j.applthermaleng.2014.02.038

Atmaca A, Yumrutaş R (2014a) Thermodynamic and exergoeconomic analysis of a cement plant: Part i - Methodology. Energy Convers Manage 79:790–798. https://doi.org/10.1016/j.enconman.2013.11.053

Atmaca A, Yumrutaş R (2014b) Thermodynamic and exergoeconomic analysis of a cement plant: Part ii - Application. Energy Convers Manag 79:799–808. https://doi.org/10.1016/j.enconman.2013.11.054

Bühler F, Nguyen T, Kjær J, Müller F, Elmegaard B (2018) Energy, exergy and advanced exergy analysis of a milk processing factory. Energy 162:576–592. https://doi.org/10.1016/j.energy.2018.08.029

Caglayan H (2018) Caliskan, H (2018) Energy, exergy and sustainability assessments of a cogeneration system for ceramic industry. Appl Therm Eng 136:504–515. https://doi.org/10.1016/j.applthermaleng.2018.02.064

Çamdali Ü, Erişen A, Çelen F (2004) Energy and exergy analyses in a rotary burner with pre-calcinations in cement production. Energy Convers Manag 45:3017–3031. https://doi.org/10.1016/j.enconman.2003.12.002

Cembureau, KEY FACTS & FIGURES / KEY FACTS. https://cembureau.eu/cement-101/key-facts-figures/. Accessed 02 April 2020

Costa VAF (2016) On the exergy balance equation and the exergy destruction. Energy 116:824–835. https://doi.org/10.1016/j.energy.2016.10.015

Darvishi H (2017) Quality performance analysis, mass transfer parameters and modeling of drying kinetics of soybean. Braz J Chem Eng 34:143–158

Fellaou S, Bounahmidi T (2017) Evaluation of energy efficiency opportunities of a typical Moroccan cement plant: part I. Energy Anal Appl Therm Eng 115:1161–1172. https://doi.org/10.1016/j.applthermaleng.2017.01.010

Fellaou S, Bounahmidi T (2018) Analyzing thermodynamic improvement potential of a selected cement manufacturing process: advanced exergy analysis. Energy 154:190–200. https://doi.org/10.1016/j.energy.2018.04.121

Fellaou S, Harnoune A, Seghra MA, Bounahmidi T (2018) Statistical modeling and optimization of the combustion efficiency in cement kiln precalciner. Energy 155:351–359. https://doi.org/10.1016/j.energy.2018.04.181

Fraga MMC, De Campos BLO, Lisboa MS, De Almeida TB, Da Costa AOS, De Lins VFC (2018) Analysis of a Brazilian thermal plant operation applying energetic and exergetic balances. Braz J Chem Eng 35:1395–1403. https://doi.org/10.1590/0104-6632.20180354s20170425

Gharagheizi F, Ilani-Kashkouli P, Mohammadi AH, Ramjugernath D (2014) A group contribution method for determination of the standard molar chemical exergy of organic compounds. Energy 70:288–297. https://doi.org/10.1016/j.energy.2014.03.124

Giannopoulos D, Kolaitis DI, Togkalidou A, Skevis G, Founti MA (2007) Quantification of emissions from the co-incineration of cutting oil emulsions in cement plants: Part II: Trace species. Fuel 86:2491–2501. https://doi.org/10.1016/j.fuel.2006.10.025

Gürtürk M, Oztop HF (2014) Energy and exergy analysis of a rotary kiln used for plaster production. Appl Therm Eng 67:554–565. https://doi.org/10.1016/j.applthermaleng.2014.03.025

Jung IH, Hudon P (2012) Thermodynamic assessment of P_2O_5. J Am Ceram Soc 95:3665–3672. https://doi.org/10.1111/j.1551-2916.2012.05382.x

Kabir G, Abubakar AI, El-Nafaty UA (2010) Energy audit and conservation opportunities for pyroprocessing unit of a typical dry process cement plant. Energy 35:1237–1243. https://doi.org/10.1016/j.energy.2009.11.003

Lazzaretto A, Tsatsaronis G (2006) SPECO: A systematic and general methodology for calculating efficiencies and costs in thermal systems. Energy 31:1257–1289. https://doi.org/10.1016/j.energy.2005.03.011

Lothenbach B, Kulik DA, Matschei T, Balonis M, Baquerizo L, Dilnesa B, Miron GD, Myers RJ (2019) Cemdata18: A chemical thermodynamic database for hydrated Portland cements and alkali-activated materials. Cem Concr Res 115:472–506. https://doi.org/10.1016/j.cemconres.2018.04.018

Madlool NA, Saidur R, Rahim NA, Islam MR, Hossian MS (2012) An exergy analysis for cement industries: An overview. Renew Sustain Energy Rev 16:921–932. https://doi.org/10.1016/j.rser.2011.09.013

Mastral F, Ceamanos J, Atienza-martínez M, Abrego J, Gea G (2018) Energy and exergy analyses of sewage sludge thermochemical treatment. Energy 144:723–735. https://doi.org/10.1016/j.energy.2017.12.007

Matschei T, Lothenbach B, Glasser FP (2007) Thermodynamic properties of Portland cement hydrates in the system CaO-Al2O3-SiO2-CaSO4-CaCO3-H2O. Cem Concr Res 37:1379–1410. https://doi.org/10.1016/j.cemconres.2007.06.002

Nat. Inst. Stand. Tech. Pesquisa para dados de espécies através da fórmula química. https://webbook.nist.gov/chemistry/form-ser/. Accessed 02 April 2020.

Ortega-Delgado B, Giacalone F, Catrini P, Cipollina A, Piacentino A, Tamburini A, Micale G (2019) Reverse electrodialysis heat engine with multi-effect distillation: Exergy analysis and perspectives. Energy Convers Manag 194:140–159. https://doi.org/10.1016/j.enconman.2019.04.056

Özilgen M (2018) Nutrition and production related energies and exergies of foods. Renew Sustain Energy Rev 96:275–295. https://doi.org/10.1016/j.rser.2018.07.055

Qian H, Zhu W, Fan S, Liu C, Lu X, Wang Z, Huang D, Chen W (2017) Prediction models for chemical exergy of biomass on dry basis from ultimate analysis using available electron concepts. Energy 131:251–258. https://doi.org/10.1016/j.energy.2017.05.037

Querino MV, Machado RAF, Marangoni C (2019) Energy and exergetic evaluation of the multicomponent separation of petrochemical naphtha in falling film distillation columns. Braz J Chem Eng 36:1357–1365. https://doi.org/10.1590/0104-6632.20190363s20180379

Ramos VF, Pinheiro OS, Ferreira da Costa E, Souza da Costa AO (2019) A method for exergetic analysis of a real kraft biomass boiler. Energy 183:946–957. https://doi.org/10.1016/j.energy.2019.07.001

Renó MLG, Torres FM, Da Silva RJ, Santos JJCS, Melo MDLNM (2013) Exergy analyses in cement production applying waste fuel and mineralizer. Energy Convers Manag 75:98–104. https://doi.org/10.1016/j.enconman.2013.05.043

Rivero R, Garfias M (2006) Standard chemical exergy of elements updated. Energy 31:3310–3326. https://doi.org/10.1016/j.energy.2006.03.020

Shahin H, Hassanpour S, Saboonchi A (2016) Thermal energy analysis of a lime production process: Rotary kiln, preheater and cooler. Energy Convers Manag 114:110–121. https://doi.org/10.1016/j.enconman.2016.02.017

Smith JM, Van Ness HC, Abbott MM (2007) Introdução à Termodinâmica da Engenharia Química. 7. ed. LTC.

Som SK, Datta A (2008) Thermodynamic irreversibilities and exergy balance in combustion processes. Prog Energy Combust Sci 34:351–376. https://doi.org/10.1016/j.pecs.2007.09.001

Song G, Xiao J, Zhao H, Shen L (2012) A unified correlation for estimating specific chemical exergy of solid and liquid fuels. Energy 40:164–173. https://doi.org/10.1016/j.energy.2012.02.016

Szargut J (1989) Chemical Exergies of the Elements. Appl Energy 32:269–286. https://doi.org/10.1016/0306-2619(89)90016-0

Terehovics E, Veidenbergs I, Blumberga D (2017) Energy and exergy balance methodology Wood chip dryer. Energy Procedia 128:551–557. https://doi.org/10.1016/j.egypro.2017.09.008

Thermal energy consumption—weighted average. (2016). https://www.wbcsdcement.org/GNR-2016/world/GNR-Indicator_93DWGck-world-2016.html. Accessed 02 April 2020

Ustaoglu A, Alptekin M, Akay ME (2017) Thermal and exergetic approach to wet type rotary kiln process and evaluation of waste heat powered ORC (organic Rankine cycle). Appl Therm Eng 112:281–295. https://doi.org/10.1016/j.applthermaleng.2016.10.053

Vučković GD, Stojiljković MM, Vukić MV, Stefanović GM, Dedeić EM (2014) Advanced exergy analysis and exergoeconomic performance evaluation of thermal processes in an existing industrial plant. Energy Convers Manag 85:655–662. https://doi.org/10.1016/j.enconman.2014.03.049

Yildirim N, Genc S (2017) Energy and exergy analysis of a milk powder production system. Energy Convers Manag 149:698–705. https://doi.org/10.1016/j.enconman.2017.01.064

Zhao Y, Wang S, Ge M, Li Y, Yang Y (2018) Energy and exergy analysis of thermoelectric generator system with humidified flue gas. Energy Convers Manag 156:140–149. https://doi.org/10.1016/j.enconman.2017.10.094